Extreme Mechanics Letters 33 (2019) 100572

Contents lists available at ScienceDirect

Extreme Mechanics Letters

journal homepage: www.elsevier.com/locate/eml

Fast healing of ionic bonds in tough hydrogels under an acoustic excitation

Hyun-Hee Lee [a], Yong-Woo Kim [a], Jaesung Woo [a], Haedong Park [d], Kahyun Hur [d], Zhigang Suo [c,*], Jeong-Yun Sun [a,b,**]

[a] Department of Materials Science and Engineering, Seoul National University, Seoul 151-742, South Korea
[b] Research Institute of Advanced materials (RIAM), Seoul National University, Seoul 151-744, South Korea
[c] John A. Paulson School of Engineering and Applied Sciences, Kavli Institute for Nanobio Science and Technology, Harvard University, Cambridge, MA 02138, USA
[d] Center for Computational Science, Korea institute of Science and Technology, Seoul 136-791, South Korea

ARTICLE INFO

Article history:
Received 30 July 2019
Received in revised form 18 September 2019
Accepted 23 September 2019
Available online 25 September 2019

Keywords:
Hydrogel
Fast healing
Recovery
Poly acrylamide/alginate hybrid gel
Ionic crosslinking
Sonication
Ultrasound

ABSTRACT

A hydrogel of covalently crosslinked chains and ionically crosslinked chains has exhibited high toughness. Under deformation, the covalently crosslinked network remains intact, and the ionically crosslinked network dissipates energy by breaking the ionic bonds. Because the broken ionic bonds can reform spontaneously, the damaged hydrogel can recover its initial state. However, the healing process of dissociated ionic bonds is slow. This paper shows that the healing process of dissociated ionic bonds accelerates under ultrasound radiation. Ultrasound enhanced the mobility of the dissociated chains, resulting in fast recovery of the mechanical properties. While a damaged gel thermally recovered 5 % of its energy density at room temperature in an hour, 37 % of the energy density was recovered using ultrasound in the same period. Molecular dynamic simulations were also included in this study to reveal the effect of ultrasound.

1. Introduction

Hydrogel is a mixture between polymer networks and water; hydrophilic polymer chains are crosslinked with each other, making empty space in which the water can be contained. Hydrogels generally show distinctive features, such as fine biocompatibility, swelling behavior under specific environments and elastomeric behavior. Therefore, hydrogels have been used in various applications, such as microfluidics [1], bioinspired devices [2,3], scaffolds for tissue engineering [4], drug delivery systems [5] and ionic actuators [6–8].

During the development of hydrogel applications, deficiencies in the mechanical properties of hydrogels have steadily raised concerns [9]. Because hydrogels mostly consist of water, most hydrogels have low stiffness and toughness. To enhance the mechanical properties, researchers have synthesized many hydrogels with toughening mechanisms [10–14]. Among them, polyacrylamide (PAAm) / alginate hybrid hydrogels have attracted interest due to their high toughness and stretchability [12,15,16]. Under deformation, the covalently crosslinked PAAm chains stabilize the deformation in the background and the ionically crosslinked alginate chains dissipate energy by breaking their ionic bonds. Because the broken ionic bonds can be healed spontaneously, the process of energy dissipation is repeatable. However, the healing process is very slow, typically a damaged hybrid gel recovers 5% its energy density at room temperature in an hour. The healing process of broken ionic bonds between alginate chains and calcium ions occurs when debonded alginate chains diffuse to another alginate chains and interact via Ca^{2+}-induced electrostatic forces.

Ultrasound is known to create microcavities in a solution, providing kinetic energy to water molecules near the cavities [17–19]. Because polymer chains in a hydrogel are hydrophilic, they could interact with water molecules dynamically. Thus, microscale energy supplied by ultrasound may enhance the mobility of the alginate chains to accelerate the healing process of the ionic bonds between the alginate chains and calcium ions. Here, we report a way to accelerate the healing process of dissociated ionic bonds by applying ultrasound. The effect of ultrasound on the healing process was experimentally investigated, and molecular dynamics (MD) simulations were also conducted to reveal the mechanism of fast healing.

---

* Corresponding author.
** Corresponding author at: Department of Materials Science and Engineering, Seoul National University, Seoul 151-742, South Korea.
E-mail addresses: suo@seas.harvard.edu (Z. Suo), jysun@snu.ac.kr (J.-Y. Sun).

https://doi.org/10.1016/j.eml.2019.100572

2. Experimental

2.1. Preparation of the hybrid gels

Polyacrylamide/alginate hybrid hydrogels were prepared by synthesizing two types of crosslinked networks at the same time. PAAm networks were covalently crosslinked using radical polymerization, and alginate networks were ionically crosslinked using calcium ions. Alginate powder (FMC biopolymer, LF 20/40) and acrylamide monomer (AAm) (Sigma Aldrich, A8887) were dissolved in DI water; 0.0225 and 0.1355 wt% with respect to the water were used, respectively. N,N -methylenebisacrylamide (MBAA) (Sigma Aldrich, M7279), 0.0006 wt% with respect to the AAm monomer, was added to covalently crosslink the AAm. Ammonium persulfate (APS) (Sigma Aldrich, A9164), 0.16 wt% with respect to the AAM monomer, was added in the solution as a thermal initiator for the AAm polymerization. The solution was degassed in a vacuum chamber, and N,N,N',N' –tetramethylethylenediamine (TEMED) (Sigma Aldrich, T7024), 0.25 wt% with respect to the AAm monomer, was added as an accelerator. A calcium sulfate slurry ($CaSO_4 \cdot 2H_2O$) (Sigma Aldrich, 31221), which functioned as the ionic crosslinker at 0.1328 wt% with respect to the alginate, was also added. The solution was poured into a glass mold and covered with a glass plate. The gels were cured in an ultraviolet crosslinker (UVP, UV crosslinker SW) with a wavelength of 254 nm and a power of 8 W for 2 h. The gels were stored in a humidity box for a day at room temperature to finish the ionic crosslinking.

2.2. Mechanical tests

Mechanical tests of the PAAm/alginate hybrid gels were carried out using a mechanical test apparatus (Instron®, 3342 machine) with a 500 N load cell. For the compression tests, the gel was synthesized in a 70×70×3 mm^3glass mold and cut with a laser cutter (Universal Laser System, VLS3.50). The compression tests were conducted using disk-shaped hybrid gels with a 10 mm diameter and 3 mm thickness. Each specimen of the gel was compressed to 90% compressive strain. The speed of compression was 1 mm/min. For the tensile tests, hybrid gels with a size of 40×14×7 mm^3 were prepared. Acrylic plates were glued with a superglue to provide stiff grip areas for the tensile tests. The 20×14×7 mm^3gel samples were loaded uniaxially after gluing. The speed of tensile stretching was 10 mm/min.

2.3. Healing tests

Damaged gels were prepared by unloading the samples after being subjected to 90% compressive strain. The gels were then submerged in 10 ml of DI water or aqueous solutions of $CaCl_2$. The gels were sonicated in a conical tube (15 ml, Falcon) by using a 6.4 mm diameter sonication tip. The distance between sonication tip and sample was around 3 cm during the operation. The sonication processes were conducted using a sonicator (Sonics&Materials, VCX-130) with a power of 26 W and a frequency of 20 kHz. The sonication time and concentrations of the $CaCl_2$ solutions were varied.

2.4. Molecular dynamics simulations

We employed molecular dynamic (MD) simulations to calculate the effect of sonication on the hybrid gel healing process. The simulation results were verified against actual experiment values. When the aqueous gels were sonicated with a frequency of 20 kHz, multiple bubbles of different sizes were generated. The bubbles, when sonication was applied, shrank and expanded repeatedly to deliver energy to the surroundings. The radii of these bubbles could be expressed using the Rayleigh–Plesset equation [20], and the velocity of the surrounding water molecules could be estimated from the changes in the bubble radii. To calculate the radii of the bubbles, the Rayleigh–Plesset equation was solved under the corresponding conditions.

$$\rho\left(R\ddot{R}+\frac{3}{2}\dot{R}^2\right)=p_{gas}\left(t\right)-P_0-P\left(t\right)-4\mu\frac{\dot{R}}{R}-\frac{2S}{R}+\frac{R}{c}\frac{dp_{gas}\left(t\right)}{dt} \tag{1}$$

$$P\left(t\right)=-P_a\sin\left(\omega t\right) \tag{2}$$

$$p_{gas}\left(t\right)=\left(P_0+\frac{2S}{R_0}\right)\left(\frac{R_0^3-h^3}{R^3\left(t\right)-h^3}\right)^{\gamma} \tag{3}$$

The surface tension, density and viscosity of water were assumed as $S = 72.8 \times 10^{-3}$ N/m, $\rho = 1000$ kg/m^3 and $\mu = 1.002 \times 10^{-3}$ Pa s. The adiabatic index and hard core value of argon were $\gamma = 5/3$ and $h = R_0/8.86$. The bubbles gas were considered to be argon because argon was the only remaining constituent gas among the initial air bubbles [21]. Parameters relating the sound, the speed of sound $c = 1500$ m/s and ultrasound angular velocity $\omega = 2\pi f$, where frequency $f = 1/T = 26.5$ kHz, were applied.

The damaged hybrid gel and its surrounding system were modeled using the typical MD software, GROMACS [22], with Gromos54A7 force fields [23]. Five types of alginate chains were prepared: $M_2G_4M_2$, $M_2G_{16}M_2$, $M_2G_{12}M_4G_4M_4G_{12}M_2$, $5(M_2G_{16}M_2)$, and $10(M_2G_{16}M_2)$, where M and G are (1-4)-linked β-D-mannuronate and its C-5 epimer α-L-guluronate residues, respectively. Simulation box sizes were set to (15×8×8 nm), (17×8×8 nm), (30×16×16 nm), (40×20×20 nm), and (40×24×20 nm), respectively. All the systems were solvated with SPC [24] water molecules and minimized using a steepest descent algorithm. MD simulations with NVT and NPT [25,26] ensembles were further performed for 0.2 ns with a 0.5 fs time step at three different temperatures, 298 K, 318 K, and 318 K, with sonication. The Verlet cut-off scheme [27] and xyz-periodic boundary condition were used. The particle-mesh Ewald (PME) method for long-range electrostatics was applied with a 1.0 nm real-space cut-off. The short-range van der Waals cut-off was set to 1.0 nm. To obtain the mobility of the alginate chains under sonication, the initial velocity of the water molecules was set to the value calculated using the Rayleigh–Plesset equation. In the other two cases in the absence of sonication, the initial water velocity was randomly set according to the temperature.

3. Results and discussion

The PAAm/alginate hybrid gel exhibited high toughness and stretchability [12]. As shown in Fig. 1a, the hybrid gel consisted of two polymer networks: the MBAA-induced covalently crosslinked PAAm network, and the Ca^{2+}-induced ionically crosslinked alginate network. The two polymer networks interpenetrated, in topological entanglement. When the hydrogel was deformed, the PAAm network remained intact, but the alginate chains and the calcium ions could dissociate (Fig. 1b). After unloading, the PAAm network returned to their original structure, whereas the alginate network was still in a dissociated state (Fig. 1c). Although the gels regained their initial configuration after unloading due to the elasticity of the PAAm network, the dissociated ionic bonds remained broken, lowering the stiffness. The hydrogel was referred to as ‘damaged’. Since the ionic crosslinks between the calcium ions and alginate chains could reform, the hybrid gel could heal after unloading. The recovery and reformation of the ionic crosslinks occurred thermally over time; however, it took a

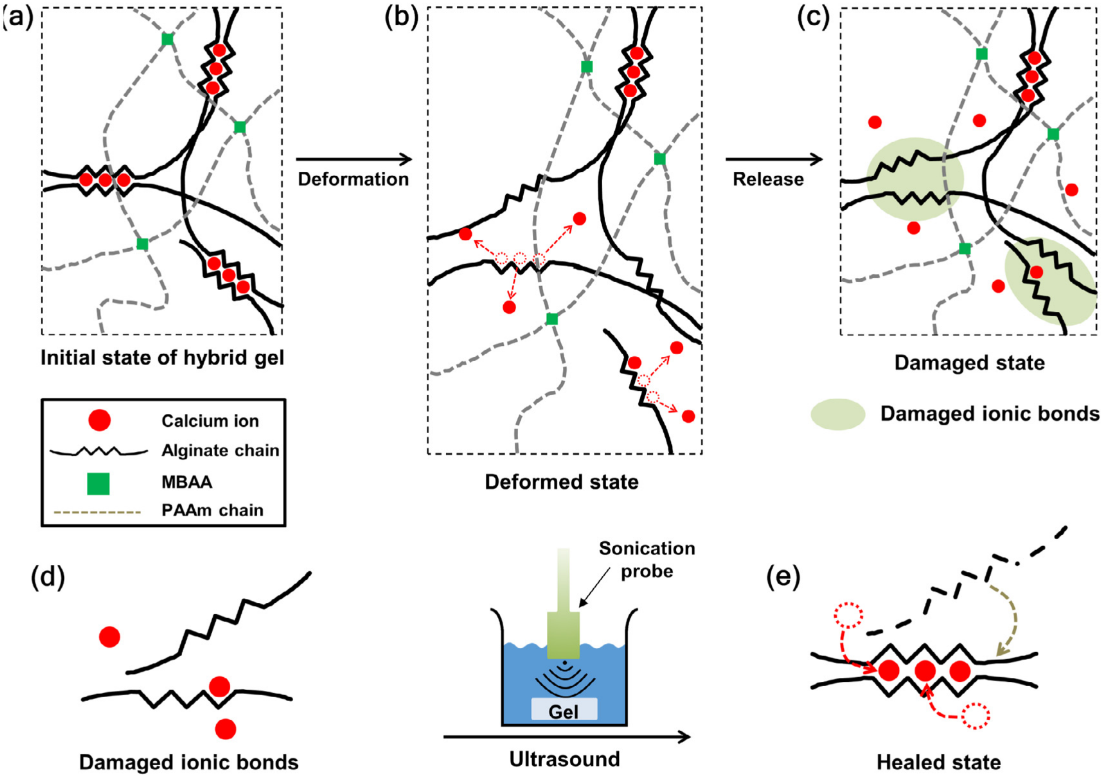

Fig. 1. Fast healing process of PAAm/alginate hybrid gels using ultrasound. (a) PAAm/alginate hybrid hydrogel consisting of covalently crosslinked polyacrylamide network and ionically crosslinked alginate network. (b) Ionically crosslinked alginate network loses its crosslinks under deformation after the calcium ions and alginate chains dissociate. (c) The calcium ions and alginate chains remain dissociated after the strain is released, decreasing the stiffness of the gel. (d) Dissociated chains and calcium ions are very slowly recrosslinked at room temperature. (e) Sonication accelerates the recrosslinking process between the alginate chains and calcium ions, causing fast healing of the PAAm/alginate hybrid gel.

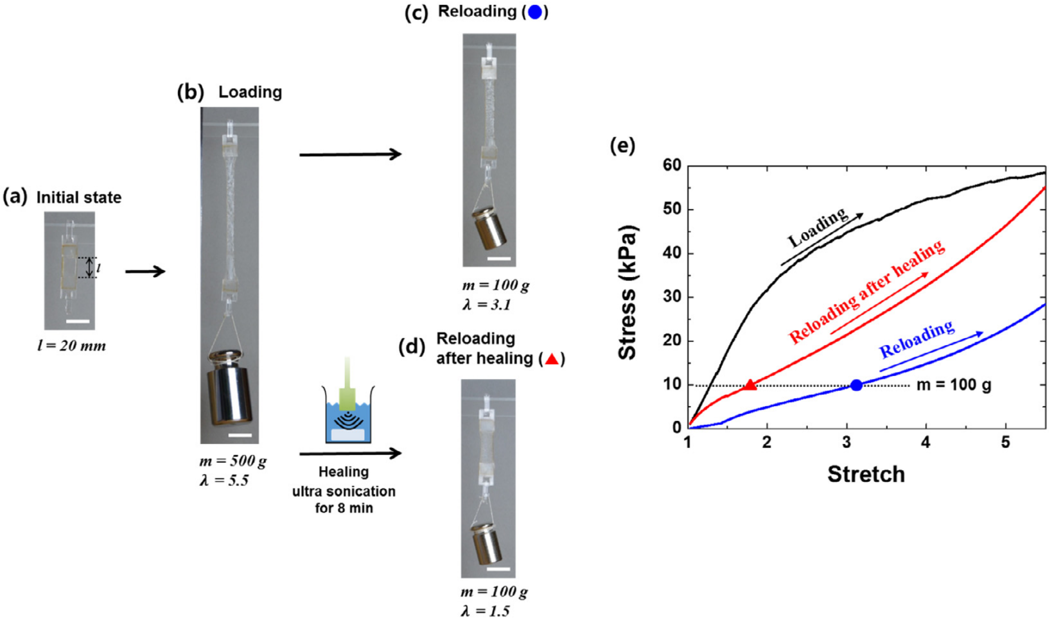

Fig. 2. The stiffness of the PAAm/alginate hybrid gel was restored after sonication. The stretch tests were conducted using gels with dimensions of 40×14×7 mm^3. (a) The gel was glued to an acrylic plate leaving 20 mm of the initial length free and was hung in the air. (b) A 500 g dead weight made the gel stretch 5.5 times its initial length during the first loading, which damaged the gel. (c) After unloading, the damaged gel was reloaded directly with a 100 g dead weight, causing the gel to stretch 3.1 times its initial length. (d) The damaged gel was sonicated for 8 min in a CaCl$_2$ 8 mM aqueous solution after unloading and was reloaded with a 100 g dead weight causing the gel to stretch 1.5 times its length. (e) Stress–stretch curves of loading, reloading and reloading after healing. The blue circle and red triangle indicate stretching with the same dead weight of 100 g representing (c) and (d), respectively. The scale bars of (a) to (d) are 2 cm.

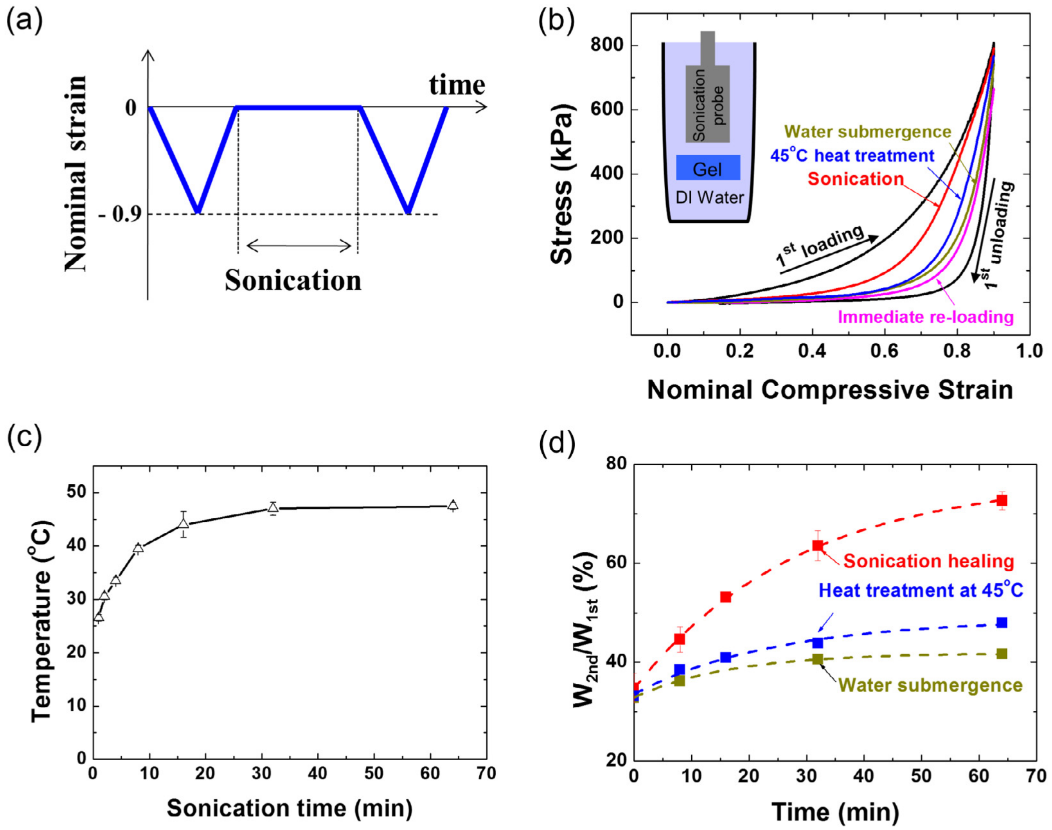

Fig. 3. PAAm/alginate hybrid gel healing process with sonication in DI water. (a) The hybrid gel was compressed up to 90% of the initial length and released, damaging the gel. The damaged gel was reloaded after healing using sonication. (b) Loading cycle and reloading curves of the hybrid gel. Before reloading the gels, water submergence at room temperature, heat treatment at 45 °C, and sonication with 26 W of power were applied separately for 64 mins. Compared to heat treatment and water submergence, sonication resulted in distinctive healing features. (c) Sonication with 26 W of power increased the temperature of 10 ml of DI water to approximately 45 °C . (d) The recovery rate indicates the efficiency of the sonication process.

long time for the stiffness of the damaged gel to recover at room temperature. Sonication accelerated the recrosslinking speed of the alginate networks (Fig. 1d-e).

Fig. 2 shows the stiffness recovery of the PAAm/alginate hybrid gels after ultrasonication. The gel, which was 20 mm long with a 98 mm^2 cross-sectional area, was hung in the air (Fig. 2a). The gel was loaded with a 500 g dead weight and stretched 5.5 times its length. (Fig. 2b). After unloading, the gel was reloaded under two different conditions. One gel was reloaded immediately after unloading, and the other gel was reloaded after sonication for 8 min in an 8 mM $CaCl_2$ aqueous solution. Since the hybrid gel was damaged during loading, the gel became soft, and reloading a 100 g dead weight made the gel stretch 3.1 times its length (Fig. 2c). In contrast, the gel that was sonicated for 8 min in the 8 mM $CaCl_2$ aqueous solution was stretched to 1.5 times its length with the same dead weight. (Fig. 2d). The stretch after sonication was similar to that of the undamaged gel, which stretched 1.3 times using the same dead weight. Fig. 2e shows the tensile stress–stretch curves. The hybrid gel was loaded to 5.5 times its length and unloaded using the tensile machine. The damaged gel was stretched using 10 kPa, which is the stress of a 100 g dead weight on a 98 mm^2 cross-sectional area, causing the gel to stretch 3.1 times and 1.7 times its length, without and with sonication for fast healing, respectively.

Prior studies [19,28,29] have proven that sonication help particles to diffuse through membranes, such as lipid bilayer and polymeric membranes. Randomly produced air-bubbles shake the molecules physically across membranes, such as lipid bilayer and polymeric membranes, enhancing the transmembrane pressure and diffusivity. Sonication can enhance the recrosslinking process of debonded alginate chains with the similar shaking process.

Sonication assisted the recovery of the damaged PAAm/alginate gel and accelerated the speed of recovery compared to the thermally healed hydrogel (Fig. 3). The sequential procedure of the loading and reloading experiments was conducted as follows (Fig. 3a). The disk-shaped hybrid gels with a 10 mm diameter and 3 mm thickness were compressed up to 90% of their initial length and then released. Sonication was carried out using the damaged gel to initiate the fast recovery process after unloading. Then, the sonicated gel was reloaded up to 90% compressive strain. Fig. 3b shows the first loading/unloading cycle and reloading curves after water submergence, heat treatment at 45 °C and sonication, which occurred for 64 mins. The immediately reloaded hybrid gels exhibited weakened stiffness, similar to the first unloading curve. The weakening was attributed to the inability of the dissociated ionic bonds between the alginate chains and calcium ions to recover. The weakened stiffness was recovered very slowly after a 45 °C heat treatment or water submergence. In contrast, sonication for the healing process recovered the stiffness of the damaged hybrid gel remarkably fast. Since ionic bond recrosslinking is a diffusion-based process, which is largely affected by temperature, the elevated temperatures in the DI water due to sonication were investigated. Sonication provides shaking energy to the alginate chains, but it also raises the water temperature. With a given sonication power of 26 W, the water temperature increased to 45 °C (Fig. 3c). Therefore, 45 °C heat treatment was conducted as a comparison in order to separate the shaking effect from the thermal effect. The recovery rates of the strain energy are plotted in Fig. 3d. The gel damaged by 90% compressive loading could only store approximately 35% of the strain energy of the initial loading during immediate reloading. The recovery rates

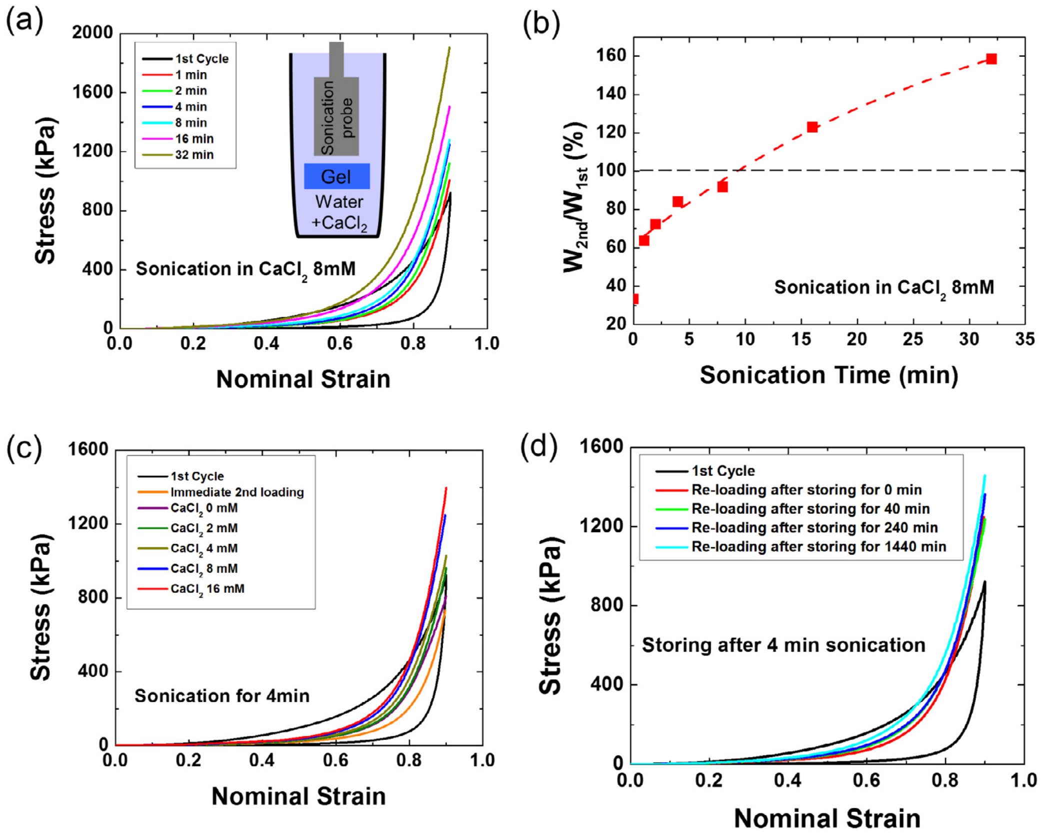

Fig. 4. The existence of calcium ions in the solution increased healing speed dramatically. The sonication process to induce healing was conducted in a calcium chloride aqueous solution. Reloading tests of the damaged hybrid gels were conducted after sonication in $CaCl_2$ aqueous solutions. (a) The sonication times were varied from 1 min to 32 min, and the (b) recovery rates after sonication in 8 mM $CaCl_2$ solutions. (c) The sonication was conducted for 4 min at different concentrations, as labeled. (d) The gels were stored in a humidity box for 40, 240, and 1440 mins after 4 min of sonication in an 8 mM $CaCl_2$aqueous solution. Additional storage in a humidity box without sonication did not result in notable differences.

continually increased with time and were proportional to the square root of time because the recovery process was based on thermal diffusion. In cases of heat treatment at 45 °C and water submergence, the recovery speed of the damaged gel was very slow. The thermal energy from the heat treatment enhanced the recovery rates but not notably. The damaged gel recovered by 5% and 12% using water submergence and heat treatment at 45 °C, respectively. In comparison, sonication accelerated the recovery speed, regaining 37% of the initial energy density within 64 mins.

The supplement of calcium ions during sonication solution significantly enhanced the healing speed. Because the formation of ionic bonds between the alginate chains and calcium ions was a reversible process, the dissociation of ionic bonds increased the number of crosslinkable alginate chains. In this environment, the existence of the ionic crosslinker affected the recovery speed. The sonication-based healing process was conducted in an 8 mM $CaCl_2$ aqueous solution instead of DI water (Fig. 4a). The damaged gel was evidently recovered after a single minute of sonication in the Ca^{2+}environment. The stiffness recovery continually and constantly increased with the increasing sonication time. After 32 min of sonication in the Ca^{2+}solution, the gel could endure almost twice the stress than that induced at the initial state at 90% compressive strain. The energy recovery rates are plotted in Fig. 4b. The 73% energy recovery occurred after 2 mins. Compared to that result, a recovery value of 72% was accomplished after 64 min of sonication in DI water; hence, sonication in the Ca^{2+} solution accelerated the speed of healing. The ratio continually increased, and the gel hyper recovered (more than 100%) after 10 min of sonication in the 8 mM Ca^{2+} aqueous solution. The recovery rate reached 160% of the initial loading after 32 min of sonication in the Ca^{2+}condition.

Although the existence of Ca^{2+} in the sonication solution dramatically increased the recovery speed, the key for achieving fast healing was the sonication process. A sonication time of 4 min was used with various concentrations of $CaCl_2$ during the healing process (Fig. 4c). Generally, the higher the Ca^{2+}concentration was, the more the stiffness recovered. However, sonication in 8 mM and 16 mM Ca^{2+} solutions recovered the damaged gel without large differences. That is, in a Ca^{2+}-rich environment, the sonication time was the dominant variable rather than the Ca^{2+} concentration. In addition, after sonication the samples were stored in DI water in order to check the effect of the abundant Ca^{2+}supply. The gel damaged by 90% compression was sonicated in an 8 mM $CaCl_2$ solution for 4 min and stored in a humidity box for further recovery (Fig. 4d). As a result, additional storing time in a humidity box did not significantly affect the recovery. Additional storage times of 0, 40, 240 and 1440 min recovered the gel as slowly as using the thermal healing process with water submergence, as shown in Fig. 3b. Thus, the existence of calcium ions in the solution simply assisted the fast recovery process by sonication. The major key of the fast recovery process of the PAAm/alginate hybrid gels was sonication.

We employed MD simulations to clarify the effects of sonication on mobility of the alginate chains. Sonication is known to supply energy to adjacent water molecules, causing the cavities to collapse [20,30,31]. In other words, the water molecules near cavities are mainly affected by the expansion and contraction of the bubbles. Consequently, the linear velocity of the water molecule was assumed to be approximately proportional to the gradient of the bubble radius (Fig. 5a). The bubble radius was calculated using the abovementioned initial conditions and the Rayleigh–Plesset

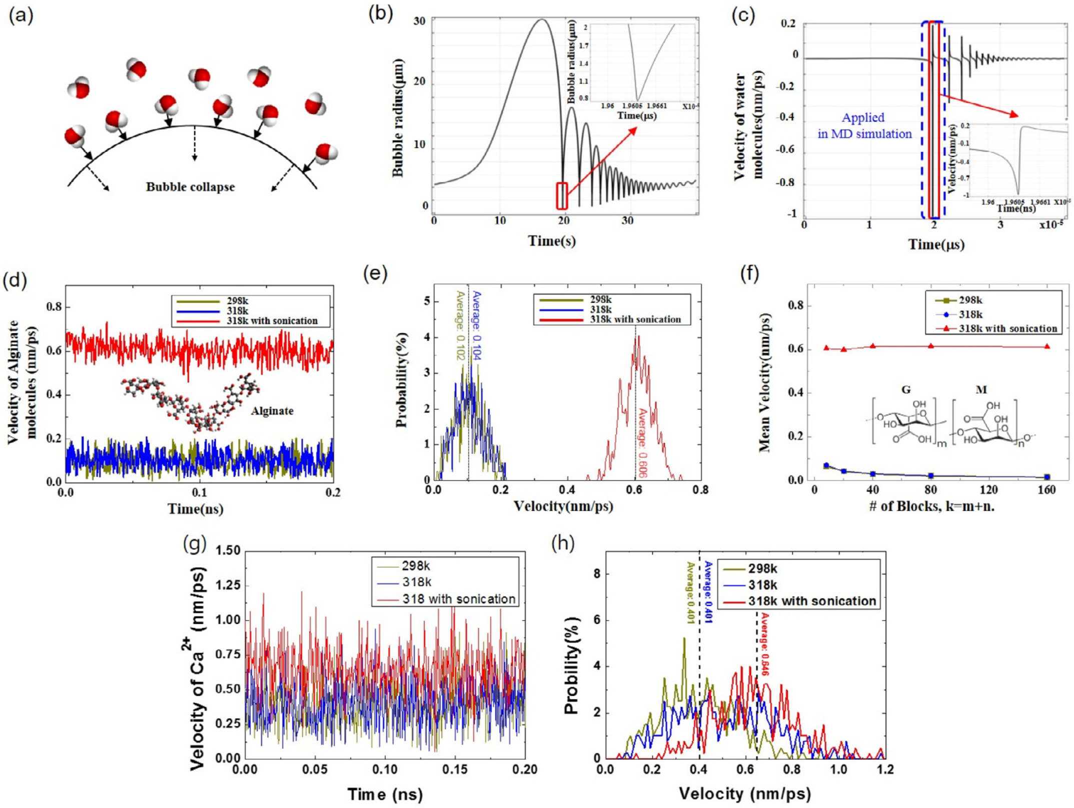

Fig. 5. Molecular Dynamics simulation was conducted to calculate the mobility of the alginate chains and calcium ions under a sonication. The sonication accelerated water molecules by growth and collapse of microbubbles. (a) The water molecules near the bubble were accelerated by the collapsing cavities. Then, the velocity of the water molecules was assumed to be proportional to the gradient of the bubble radius. Among the numerous cycles, the first cycles after single sonication were considered for calculating the water velocity due to continuous sonication treatment. (b) The radius of the bubble and (c) the water velocity were calculated using the Rayleigh–Plesset equation. (d) The velocity of one alginate chain composed of 8 blocks was calculated as a function of time. (e) The velocity distribution of alginate. (f) The mean velocity was calculated for various lengths of the alginate chains. (g) The velocity of calcium ions as a function of time. (e) The velocity distribution of calcium ions.

equation, which corresponded to the single sonication treatment, Eq. (1)–(3). In Fig. 5b, the bubble radius is plotted for a single sonication treatment. In particular, the first cycle of expansion and contraction was mainly used to determine the behavior of the water molecules because the sonication was continuously applied. Thus, the velocity of the water molecules could be obtained from the gradient of the first minimum peak of the bubble radius (Fig. 5c). The water velocity under sonication was approximately 1 km/s, as driven from the high-energy acoustic microcavitation.

Generally, the temperature of the solution affected the mobility of the molecules in the solution. However, as shown above, the temperature changes by themselves were insufficient to heal the gel. To verify the influence of the two factors on healing, MD simulations of three conditions corresponding to the experiments were conducted. The water velocity under sonication was applied using an MD simulation program (GROMACS) to provide the initial conditions. As shown in Fig. 5d and e, the velocity of one alginate chain composed of 8 blocks was calculated as a function of sonication time. The alginate chain mobility was obviously improved during sonication. Compared with the experiments without sonication, the alginate chains exhibited a 6-times faster linear velocity. In contrast, as with the experiment results, the temperature effect on the mobility was negligible (Fig. 5d and e). In addition, the simulations were carried out while increasing the length of the alginate chains as shown in Fig. 5f. Interestingly, the sonication identically improved the mobility of the alginate molecules regardless of the chain length. As shown in Fig. 5f, under sonication, the mean velocities were increased to approximately 0.6 nm/ps for all lengths. However, the speed of the alginate chains without any treatment tended to decrease with the increasing chain length. In Fig. 5g and h, the mobility of calcium ions is plotted. The mobility of calcium ions is enhanced from 0.401 nm/ps to 0.646 nm/ps by the sonication. Under a sonication, calcium ions are slightly faster than alginate chains but the mobility of them are comparable. Therefore, we concluded that enhanced mobility of alginate chains by the sonication dominantly play a role to reduce the recovery time of the damaged hybrid gel.

4. Conclusion

Sonication assisted the recrosslinking process of alginate chains and calcium ions, accelerating the recovery of the damaged gels. In particular, since the existence of calcium ions supported the recovery of damaged PAAm/alginate hybrid gels, they became fully recovered within several minutes in a calcium-rich environment. Also, we clarified the effects of sonication and temperature on the healing process using MD simulations. These results can also be used for other ionically crosslinked hydrogels. Previous time-consuming healing processes can be replaced with the sonication method described herein, which takes only a few minutes to achieve complete healing.

Declaration of competing interest

The authors declare that they have no known competing financial interests or personal relationships that could have appeared to influence the work reported in this paper.

Acknowledgments

This work was supported by a National Research Foundation of Korea (NRF) grant funded by the Korean Government (NRF-2018M3A7B4089670). ZS acknowledge the support of MRSEC, USA (DMR-14-20570).

References

[1] D.J. Beebe, et al., Functional hydrogel structures for autonomous flow control inside microfluidic channels, Nature 404 (6778) (2000) 588–590.

[2] L. Dong, et al., Adaptive liquid microlenses activated by stimuli-responsive hydrogels, Nature 442 (7102) (2006) 551–554.

[3] A.S. Hoffman, Hydrogels for biomedical applications, Adv. Drug Deliv. Rev. 64 (2012) 18–23.

[4] K.Y. Lee, D.J. Mooney, Hydrogels for tissue engineering, Chem. Rev. 101 (7) (2001) 1869–1880.

[5] Y. Qiu, K. Park, Environment-sensitive hydrogels for drug delivery, Adv. Drug Deliv. Rev. 64 (2012) 49–60.

[6] J.Y. Sun, et al., Ionic skin, Adv. Mater. 26 (45) (2014) 7608–7614.

[7] C. Keplinger, et al., Stretchable, transparent, ionic conductors, Science 341 (6149) (2013) 984–987.

[8] M.E. Harmon, M. Tang, C.W. Frank, A microfluidic actuator based on thermoresponsive hydrogels, Polymer 44 (16) (2003) 4547–4556.

[9] K.S. Anseth, C.N. Bowman, L. Brannon-Peppas, Mechanical properties of hydrogels and their experimental determination, Biomaterials 17 (17) (1996) 1647–1657.

[10] J.P. Gong, et al., Double - network hydrogels with extremely high mechanical strength, Adv. Mater. 15 (14) (2003) 1155–1158.

[11] D.C. Tuncaboylu, et al., Tough and self-healing hydrogels formed via hydrophobic interactions, Macromolecules 44 (12) (2011) 4997–5005.

[12] J.-Y. Sun, et al., Highly stretchable and tough hydrogels, Nature 489 (7414) (2012) 133–136.

[13] W.R. Illeperuma, et al., Fiber-reinforced tough hydrogels, Extrem. Mech. Lett. (2014).

[14] Y. Okumura, K. Ito, The polyrotaxane gel: A topological gel by figure - of - eight cross - links, Adv. Mater. 13 (7) (2001) 485–487.

[15] W. Hennink, C. Van Nostrum, Novel crosslinking methods to design hydrogels, Adv. Drug Deliv. Rev. 64 (2012) 223–236.

[16] J. Li, et al., Hybrid hydrogels with extremely high stiffness and toughness, ACS Macro Lett. 3 (6) (2014) 520–523.

[17] K.S. Suslick, Sonochemistry, Science 247 (4949) (1990) 1439–1445.

[18] K.S. Suslick, The chemical effects of ultrasound, Sci. Am. 260 (2) (1989) 80–86.

[19] M.P. Sheetz, S.I. Chan, Effect of sonication on the structure of lecithin bilayers, Biochemistry 11 (24) (1972) 4573–4581.

[20] Lucas L. Vignoli, et al., Modeling the dynamics of single-bubble sonoluminescence, Eur. J. Phys. 34 (3) (2013) 679–688.

[21] M.P. Brenner, S. Hilgenfeldt, D. Lohse, Single-bubble sonoluminescence, Rev. Modern Phys. 74 (2) (2002) 425.

[22] David Van Der Spoel, et al., GROMACS: fast, flexible, and free, J. Comput. Chem. 26 (16) (2005) 1701–1718.

[23] Nathan Schmid, et al., Definition and testing of the GROMOS force-field versions 54A7 and 54B7, Eur. Biophys. J. 40 (7) (2011) 843.

[24] Herman J.C. Berendsen, et al., Interaction models for water in relation to protein hydration, in: Intermolecular Forces, Springer Netherlands, 1981, pp. 331–342.

[25] Herman J.C. Berendsen, et al., Molecular dynamics with coupling to an external bath, J. Chem. Phys. 81 (8) (1984) 3684–3690.

[26] M. Parrinello, A. Rahman, Polymorphic transitions in single crystals: A new molecular dynamics method, J. Appl. Phys. 52 (12) (1981) 7182–7190.

[27] L. Verlet, Computer experiments on classical fluids. I. Thermodynamical properties of Lennard-Jones molecules, Phys. Rev. 159 (1) (1967) 98.

[28] J.D. Floros, H. Liang, Acoustically assisted diffusion through membranes and biomaterials, 1994.

[29] D. Papahadjopoulos, et al., Studies on membrane fusion. 1. Interactions of pure phospholipid membranes and the effect of myristic acid, lysolecithin, proteins and dimethylsulfoxide, Biochim. Biophys. Acta (BBA)-Biomembranes 448 (2) (1976) 245–264.

[30] H.B. Chew, et al., Compressive dynamic scission of carbon nanotubes under sonication: fracture by atomic ejection, Proc. R. Soc. Lond. Ser. A Math. Phys. Eng. Sci. 467 (2129) (2011) 1270–1289.

[31] Nathaniel Huebsch, et al., Ultrasound-triggered disruption and self-healing of reversibly cross-linked hydrogels for drug delivery and enhanced chemotherapy, Proc. Natl. Acad. Sci. 111 (27) (2014) 9762–9767.